VIROLOGY

Lightweight multiscale early warning system for influenza A spillovers

Tommaso Alfonsi[1]†, Anna Bernasconi[1]*†, Matteo Chiara[2], Stefano Ceri[1]

Spillovers of zoonotic Influenza A viruses (IAVs) into farmed animals and humans have the potential to trigger epidemics or even global pandemics. We introduce FluWarning, a highly efficient and elegant computational method based on anomaly detection of codon bias and dinucleotide composition for early identification of divergent viral HA segments. We applied FluWarning to the 2009 influenza pandemic as a test case. FluWarning successfully identified the emergence of pdm09, the virus that caused the pandemic, with warnings preceding the observed global spread. Applied to H5N1 specimens collected between 2019 and 2025, FluWarning flagged genotypes D1.1 and B3.13, both associated with recent spillovers in dairy cows in the United States. In summary, FluWarning is an effective, lightweight, multiscale warning system for IAVs, detecting spillovers with few available sequences.

INTRODUCTION

Early detection of changes in the viral genome is critical for the development of warning systems and the implementation of mitigation strategies. Cross-species transmission events have been shown to be increasingly frequent (1) and can escalate to global health emergencies. Evolutionary breakthroughs may lead to sustainable transmission in a new ecological niche and eventually spillover to further species [as previously observed for Ebola (2) or coronaviruses (3)].

In information science, conflict and disruption are typically observed through anomaly detection methods; anomalies are carriers of critical information, such as extreme weather conditions, fault tracking, and fraud activities. Several surveys of anomaly detection methods have been proposed previously (4, 5), also for temporal data (6). In the context of genomic surveillance, these approaches can be extended to processing information carried by viral genomes such as the composition in %GC (i.e., guanine-cytosine content percentage), dinucleotide frequencies, and the preference for specific synonymous codons in protein-coding genes. The analysis of patterns of codon preference (exploiting redundant encoding of amino acid residues) was previously proposed to capture patterns of viral adaptation in influenza A viruses (7, 8). However, such analyses were retrospective and did not aim to identify the emergence of novel viral strains.

Here, we introduce FluWarning, an efficient computational approach that applies anomaly detection to genomic features, flagging viral specimens showing critical changes. We selected "stray" [Search and TRace Anomaly, (9)], a powerful unsupervised method for anomaly detection applied to high-dimensional data. Given a set of items, anomalies are defined as items whose distance gap to typical data is substantially larger than the distance between typical items.

We use genome sequences retrieved from the Global Initiative on Sharing All Influenza Data (GISAID) (10). To recognize "anomalous" sequences, the method only requires the collection date metadata and the hemagglutinin (HA) segment sequence, which is the most commonly sequenced one and modulates host specificity (11);

we collect a few additional metadata (serotype, location, genotype, and host type) to help the interpretability of the results. The method is general and adapts to any collection of Influenza A virus (IAV) sequences available at a surveillance center; the method is also multiscale, as it can detect both macroscopic events, such as the significant prevalence growth of a new clade/genotype within a large population, and microscopic events, such as individual anomalous sequences.

Computational approaches to tracking viral evolution typically focus on single mutations or groups of mutations and their predicted functional effects on epidemiology, immunology, viral dynamics, and diagnosis/treatment, to identify novel variants of concern (12). Here, we leverage codon usage bias and dinucleotide frequency to capture significant changes in genome composition. Each sequence is encoded in a 75-dimensional feature vector, and the stray algorithm is applied to detect divergent sequences, which are individually or globally assessed. FluWarning does not aim to predict evolutionary trajectories, as in other studies based on anomaly detection (13, 14), but is capable of capturing key epidemiological events at their early stage.

FluWarning is configurable by time window and geographic location of interest (from continents to local surveillance units). The method runs in a streamlined, reproducible pipeline (15). The results are organized in a user-friendly data mart (16) that allows data navigation and selection of specific countries, weeks, and infected host species.

FluWarning has been designed and validated on the paradigmatic case of the 2009 H1N1 pandemic (pdm2009), as the progression and all marker events are well known. The method was then used in the compelling case of the H5N1 influenza virus, which has recently caused an epidemic in dairy cattle in the United States (17) and might be close to reaching pandemic potential according to recent studies (18). Our work builds upon a recently published, systematic analysis of the complete collection of publicly available complete genome H5N1 sequences collected in North America (19) starting from 2019.

[1]Department of Electronics, Information, and Bioengineering, Politecnico di Milano, Via Ponzio 34/5, 20133, Milan, Italy. [2]Department of Biosciences, Università degli Studi di Milano, Via Celoria 26, 20133, Milan, Italy.
*Corresponding author. Email: anna.bernasconi@polimi.it
†These authors contributed equally to this work.

RESULTS
Data collection

From GISAID EpiFlu (10), we downloaded 3387 H1N1 specimens collected from mammalian hosts between 28 July 2008 and 10 January

2010, and 12,854 H5N1 specimens from any host between 1 January 2019 and 25 July 2025. For both datasets, we downloaded only specimens collected in North America. After our data curation pipeline (see Materials and Methods) we obtained: 3034 H1N1 sequences (96.4% from human hosts and 3.6% from swine) and 12,092 H5N1 sequences (79.6% from wild birds, 5.9% from domestic birds, 14.2% from nonhuman mammals, and 0.3% from human hosts).

Feature selection
Several studies highlighted how IAVs from different hosts display different genome compositions in terms of di-nucleotides (*20*, *21*) and codon usage preferences (*7*, *8*, *22*–*25*). The data processing pipeline computes 75 numeric features for every sequence. The first 59 features correspond to the relative synonymous codon usage (RSCU) (*26*) of all the codons, excluding the three stop codons (TAA, TAG, and TGA) and the amino acids lacking alternative synonymous codons (Met: ATG; Trp: TGG). Further, 16 features describe dinucleotide frequencies of all the permutations $P(4, 2)$, with repetitions, of the four nucleotides, normalized by genome composition.

Anomaly detection in high dimensional data
Stray (*9*) focuses on anomaly detection in high-dimensional data. In our application of stray, each item is a vector of 75 variables; items are sorted according to a total order by CollectionDate and then by AccessionID. The algorithm is applied to moving windows consisting of N items. At each new window W_i, the first item of window W_{i-1} is dropped, and the item n_i, denoted as "new item," is added as last window item; we refer to the collection date of the new item as "characteristic date" of the window. Note that the new item in the window W_i is included in the subsequent $N - 1$ windows, where it progressively scales up to becoming the first item, and then is finally removed.

In stray, an important, user-defined parameter is k; an item is deemed an outlier when the distance to its kth nearest neighbor is above a data-driven threshold, termed "gap," automatically computed (see Materials and Methods); k can be interpreted as the maximum size of microclusters detected as anomalies. For each window W_i, stray produces a vector $\mathcal{V}_i$ of N binary values v_{ij}, where $v_{ij} = 1$ indicates that item j in the window i is anomalous. Last, a window is associated with a warning if the new item is anomalous, i.e., $v_{i,N} = 1$.

Tracking viral strain replacement with stray
Figure 1A shows stray applied to 51 consecutive windows, representing a complete substitution of blue items (baseline viral population) with red items (new viral population). We consider $N = 50$ and $k = 10$; stray is executed 51 times, starting from 50 blue items (blue), progressively replaced by red items. Note that the blue item in position 1 of window 0 is discarded in window 1, making space for an item in position 50 of window 1. This item is an anomaly, as its distance from all other items is greater than a data-defined gap; all anomalies are rendered with a black triangle.

Anomalies occur only when red items, that progressively form a microcluster, are below the user-defined threshold k. Thus, anomalies progressively occur only for windows 1 through 10, all associated with a warning. At window 11, a cluster of size 11 is created, and for each red item, the 10th-neighbor distance drops; red items are no longer anomalies as they belong to a sufficiently large cluster (see Fig. 1B). Then, the substitution of blue items with red items continues, up to window 40. Here, blue items are a minority; they

create a microcluster of size 10 and become anomalies. However, as warnings are only associated to new items, no warning is thrown.

Sensitivity and specificity analysis
We prepared an ad hoc dataset with (i) N-sized baseline group (called $G1$), drawn from an initial set of 130 ordered items (called $X1$); and (ii) N-sized penetrating group (called $G2$), drawn from a different set of 100 ordered items (called $X2$). The two sets $X1$ and $X2$ represent viral sequences collected in the same epidemic year, but from different viral clades, retrieved from GISAID; individual IDs are reported in our Zenodo repository (*15*); each sequence is summarized by 75 extracted features representing its HA viral genome. We build the noise experiments by randomly replacing respectively 10, 20, or 30% of the items of $G2$ with elements of $X1$ (termed "noise items") not used in $G1$.

Table 1 reports results, with $N = (50, 100)$ and $k = (10, 15)$; a complete version of the experiments with 15 combinations of N and k is in table S1, but, as discussed in our H1N1 pandemic analysis, smaller N,k pairs are not recommended for epidemic/pandemic analyses. Each table line represents a specific combination of N, k, and noise level (percentage over $G2$ and absolute number of noise items). For each combination, we run FluWarning 50 times and average the results, collected in the last four columns, which represent the following: (i) the number of warnings, identical to k in all cases; (ii) the window number in which the last warning was detected [denoted as last warning ordinal (LWO)]; (iii) sensitivity, defined as k/LWO (i.e., the ideal LWO divided by the actual LWO, capturing the ratio of true positives over all the warnings); and (iv) specificity, defined as $(N + 1 - \text{LWO})/(N + 1 - k)$ (i.e., the ideal ordinal from which nonwarning items are detected, divided by the actual nonwarning ordinal, capturing the ratio of true negatives over all the warnings).

As expected, LWO increases with noise, while sensitivity and specificity decrease from the perfect value of 1 (no noise); nonetheless, both metrics remain acceptable even with 30% noise, showing that the method is robust. Note that, in any warning system, a few false positives are not a concern, as all sequences that triggered a warning must be further explored.

Data mart–based monitoring
FluWarning is distributed as software supporting data processing and data exploration. In data processing, the software receives a stream of sequences (e.g, downloaded from GISAID by an authorized user or provided from a surveillance laboratory). After sequence alignment, feature selection, and anomaly detection, warning-related sequences and their metadata are collected within a (SQLite) database. For data exploration, the database feeds a data mart, explorable through a web-based application (Streamlit), packaged in an easy-to-install container (Docker), see (*15*). The data mart supports the inspection of aggregate counts of warnings across selected hosts, locations, and periods, as well as the extraction of single sequences metadata; the software is developed to facilitate installation and use.

The H1N1 pandemic (2008–2009)
We used the 2009 H1N1 pandemic to identify the most appropriate settings for FluWarning for the detection of epidemiologically important events. The pdm09 virus, which caused the pandemic, originated in late 2008 in Mexico, but was first isolated and sequenced on 14 April 2009, by the Centers for Disease Control and Prevention
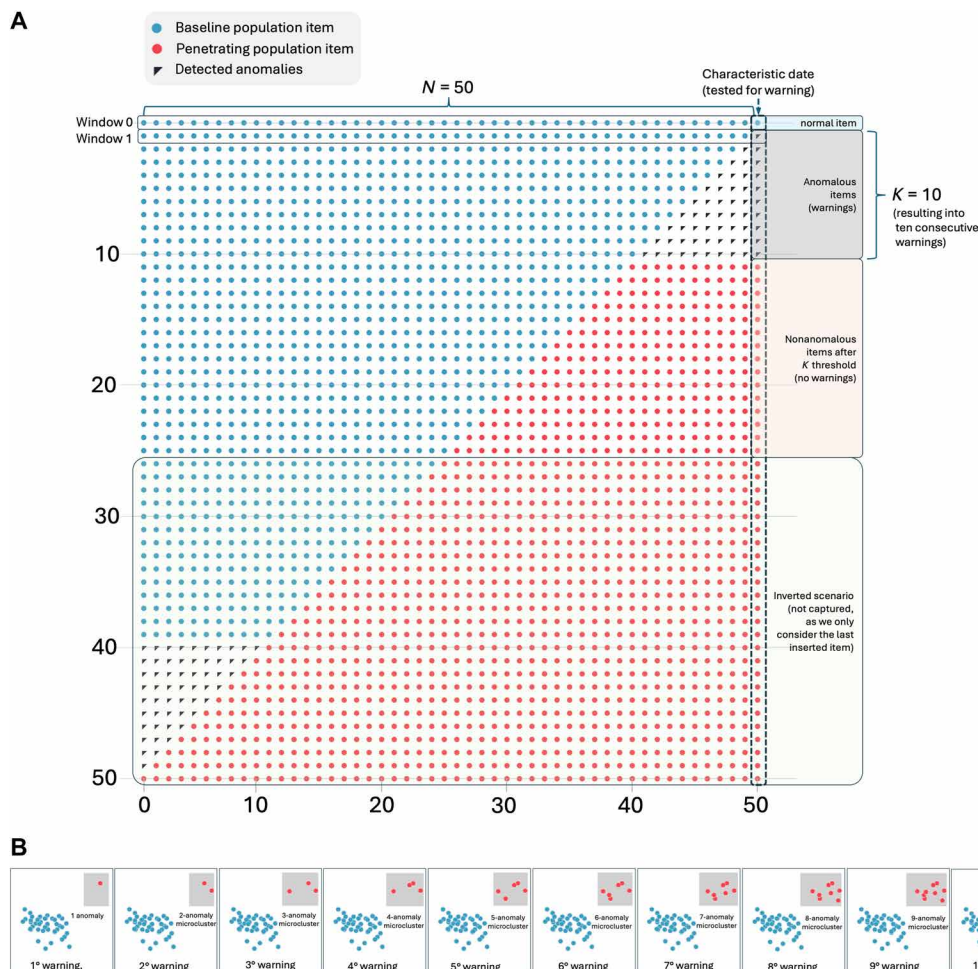
Fig. 1. Stray method explained. (**A**) Complete substitution of blue items (a baseline viral population) with red items (a new viral population). With $N = 50$ and $k = 10$, stray is executed 51 times, starting from a window that contains 50 normal items (blue). Anomalies occur only when red items, that progressively form a microcluster, are below the user-defined threshold k, then, in windows 1 through 10, all are associated with a warning. At window 11, a cluster of size 11 is created, red items cannot be considered anomalous because they have created a sufficiently large cluster. Then, the population of red items grows up to window 40, where blue items are a minority; they create a microcluster of size 10, and all blue items become anomalies. However, as we are only interested in new items (in position 50), no warning is thrown. (**B**) shows an "ideal" case where blue and red sequences are well-separated in the 75-dimensional space. Here, we capture distances on two highly representative dimensions (e.g., the two principal components after dimensional reduction). Red microclusters are recognized as anomalous until their size reaches $k = 10$.

(*27*). Following a rapid increase in flu cases associated with pdm09, the World Health Organization (WHO) declared a "public health emergency of international concern" on 25 April 2009. By June, pdm09 completely replaced other seasonal H1N1 flu strains, and the outbreak was declared a pandemic (*28*).

We analyzed 3034 H1N1 HA sequences collected from specimens infecting human hosts between August 2008 and January 2010. Data were aggregated in nonoverlapping intervals of 2 weeks. Each interval has a starting week number W_i (with incremental numbers, per year), a corresponding start date D_i, and includes all the sequences with a collection date included in the interval $[D_i, D_{i+1})$. To establish the most suitable settings for identifying the emergence of a novel virus in FluWarning, we visually inspected the total number of warnings emitted by the system at every interval W_i, according to different combinations of N and k.

As shown in fig. S1, with $N = (50, 100)$ and $k = (10, 15)$, a sharp peak of warnings was observed, specifically at intervals ranging

from 2009-11 to 2009-20. These intervals span from 12 March 2009 to 13 May 2009 and align exactly with the initial emergence and spread of pdm09. On the basis of these observations, only values of $N = (50, 100)$ and $k = (10, 15)$ were considered for epidemic/pandemic scale analyses.

We reasoned that windows W_i associated with a statistically significant increase (corrected P value ≤0.05) in the number of detected anomalies likely reflect key epidemiological events such as, for example, the emergence and spread of a new viral variant. From now on, we will refer to these windows as "super warnings." Super warnings were identified using Fisher's exact test (see Materials and Methods) by comparing the proportion of warnings emitted at a given window W_i with the overall proportion of warnings across the entire dataset. P values were corrected with the Benjamini-Hochberg procedure to control the false discovery rate. An empirical assessment (see fig. S2) indicated that super warnings can be reliably detected when an interval contains at least 20 sequences, of which six

Table 1. Sensitivity and specificity analysis, with *N* = (50, 100) and *k* = (10, 15). Each line represents a specific combination of *N* (column 1), *k* (column 2), and noise level as a percentage over *G*2 (column 3). The absolute number of noise items is also reported (column 4). For each combination, we run FluWarning 50 times; we report the number of warnings (column 5); averages of the window number in which the last warning was detected, denoted as last warning ordinal (LWO; column 6), sensitivity (column 7), and specificity (column 8).

N	k	%Noise	#Noise items	#Warnings	LWO	Sensitivity	Specificity
50	10	0%	0	10	10.00	1	1
		10%	5	10	11.16	0.901	0.972
		20%	10	10	12.68	0.798	0.935
		30%	15	10	13.84	0.736	0.906
	15	0%	0	15	15.00	1	1
		10%	5	15	16.70	0.900	0.953
		20%	10	15	18.60	0.812	0.900
		30%	15	15	21.10	0.719	0.831
100	10	0%	0	10	10.00	1	1
		10%	10	10	11.00	0.915	0.989
		20%	20	10	11.98	0.849	0.978
		30%	30	10	14.52	0.709	0.950
	15	0%	0	15	15.00	1	1
		10%	10	15	16.52	0.913	0.982
		20%	20	15	18.22	0.829	0.963
		30%	30	15	21.70	0.706	0.922

or more (≥30%) are flagged with a warning. To minimize biases introduced by uneven sampling of viral isolates (see large discrepancies in sequencing coverage in Fig. 2), we computed super warnings only for windows containing at least 20 sequences.

Results are shown in Fig. 2 (A to C). For all four configurations of stray, super warnings (see dark blue cells) were emitted from 2009-13 to 2009-21. The first pdm09 sequence in the dataset was collected on 12 March 2009 (week 2009-11) and was identified as a warning by stray in all four configurations. A super warning is instead emitted at 2009-13; by this interval of time, the number of pdm09 sequences in the GISAID database increased to 14, collected in Mexico (*n* = 7) and California (*n* = 7), consistent with the epidemiological history of the H1N1 pandemic of 2009.

Starting from week 2009-15, when pdm09 established itself as the most prevalent H1N1 clade in the dataset, the majority of the warnings emitted by the system flagged seasonal flu viral isolates. By week 2009-25, pdm09 accounted for (almost) the totality of H1N1 samples, and the number of warnings identified by stray at any subsequent intervals dropped to levels comparable to those observed before the emergence of pdm09 (see fig. S3 and data S1).

Data mart–based monitoring

To showcase the power of our data mart, consider Fig. 2D, obtained by setting *N* = 50 and *k* = 10, which illustrates the geographic locations associated with warnings. In biweek 2009-13/14 (23 March to 5 April 2009), warnings occurred in California (four warnings out of seven isolates), Mexico (2 of 7), and Illinois (1 of 1); in biweek 2009-15/16 (6 to 19 April 2009), warnings occurred in Hawaii (3 of 3), Texas (1 of 11), and Mexico (1 of 22). By week 2009-17/18 (20 April 3 May 2009), a substantial number of warnings occurred in California (25 of 108), and US-collected warnings spread to Minnesota, Kansas, New York, and Texas, marking the start of the pdm09 pandemic. Collectively, these

results indicate that FluWarning correctly recapitulates the main events of the 2009 H1N1 pandemic and flags the emergence of new viral clades/strains almost in real time. These considerations prompted us to apply the same analytical workflow to H5N1.

The H5N1 2.3.4.4b clade (2020–2025)

Highly pathogenic (HPAI) strains of H5N1 IAVs are considered a constant pandemic threat since their recurrent outbreaks in mammalian species, including sporadic cases of human infection with reported high mortality rates (*29*). Originally described and isolated in 2013–2014 in Asia, the HPAI H5N1 2.3.4.4b clade recently crossed continental barriers and became increasingly frequent in Europe, North America, and South America (*30*). Besides infecting wild and domestic birds, 2.3.4.4b was associated with several distinct spillovers to mammals throughout 2020 to 2025 and recently caused a large epidemic of avian flu in dairy cattle in the United States, raising a substantial concern for human health (*17*). Two distinct genotypes of H5N1 2.3.4.4b have caused independent spillovers of IAV to dairy cows in North America. Genotype B3.13 was responsible for a large-scale outbreak in dairy cattle in 2024; the first isolate of B3.13 was collected from a dairy cow in Texas on 13 March 2024 (*19*). More recently, in January 2025, genotype D1.1 was detected in dairy cattle in Nevada (*31*); however, this outbreak was relatively limited in scale compared with the one caused by B3.13.

We considered a total of 12,092 HA segment sequences and associated metadata of H5N1 collected between 15 September 2020, and 29 May 2025, in North America. As a side note, we extracted GISAID data up to 25 July 2025; 1097 isolates submitted in the last 3 months of 2025 had incomplete geographic and collection date metadata, and could not be evaluated. A total of 1068 distinct warnings were emitted by FluWarning in at least one of the *N* = 50, 100 and *k* = 10, 15 configurations (see fig. S4 and data S1); sequences assigned to the B3.13
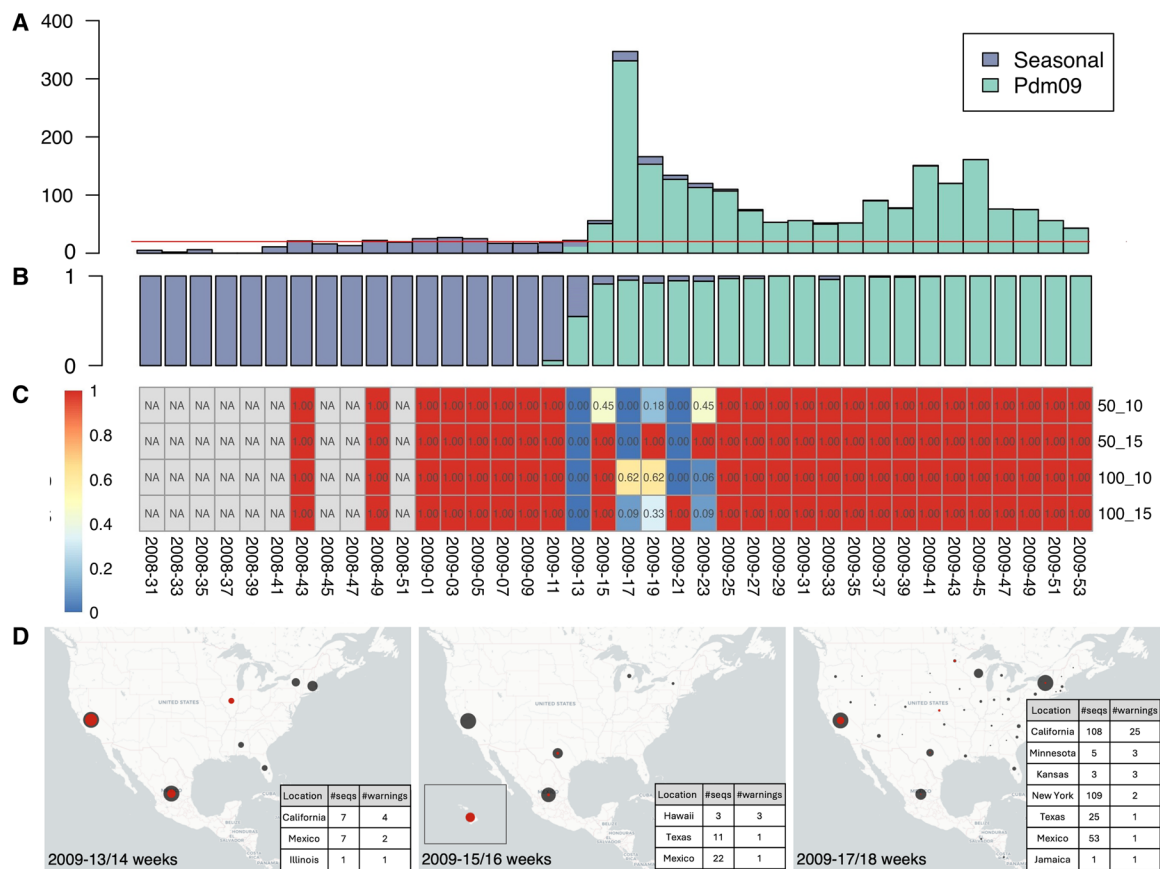
Fig. 2. Circulation of H1N1 strains from 2008-33 to 2009-53 and warnings by stray. (**A**) Barplot showing the total number of H1N1 sequences classified as "seasonal-flu" or "pdm09" in the GISAID EpiFlu database at each time interval. The red line indicates the threshold (20 sequences) used to compute super warnings. (**B**) Relative proportions (percentage with respect to the total number of sequences) of seasonal-flu and pdm09 sequences. (**C**) Heatmap (with stray settings $N = 50$, 100 and $k = 10$, 15) displaying the FDR corrected P values for the statistically significant increase in the number of warnings. Time intervals are shown on columns, parameters of stray on the rows. NA: Super warnings are not computed due to an insufficient number of sequences. (**D**) Maps drawn for North and Central America, representing warnings during the 2009-13 to 2009-17 weeks period. One can note the diffusion, initially in Mexico and Southern California (as it can be read in location metadata), up to other States of the US.

genotype accounted for 62.83% of the total number of warnings and 90.05% of the warnings emitted by FluWarning between 2024-11 and 2024-37. These windows were associated with super warnings according to all four selected configurations of stray, see Fig. 3C (complete heatmap in fig. S5). As observed from the breakdown of the circulation of 2.3.4.4b genotypes in North America, displayed in Fig. 3 (A and B), this interval aligns almost exactly with the emergence and spread of B3.13. Several other genotypes, including for example B2.1, B3.2, and B3.6, display a widespread and sustained circulation in North America (estimated prevalence ≥0.2 for more than 4 weeks) in the timeframe considered in our analyses, but none of these exhibited a statistically significant association with super warnings.

Unlike B3.13, which accounted for the majority of warnings, only 23 D1.1 sequences were collectively associated with a warning, representing approximately 0.2% of the total (data S1). However, 20 of these sequences were collected between the end of 2024 and the first half of 2025 (weeks 2024-50 to 2025-25); in this dataset, only four D1.1 sequences originate from dairy cows, of which the first one, collected in Nevada on 21 January 2025, was flagged as a warning, aligning with the observation reported in (*31*). All D1.1 warnings were detected using a window size of $N = 50$, and no warnings were detected for D1.1 with $N = 100$ (fig. S4).

As shown in Fig. 3, the configuration with $N = 50$ and $k = 10$ emitted super warnings at the end of 2024/beginning of 2025 (2024-52 to 2025-01), coinciding with the reported outbreak of D1.1 in dairy cattle in the United States. D1.1 sequences accounted for a substantial proportion (~35%) of warnings recorded across this interval of time, consistent with a super warning for this genotype. Configurations with $N = 100$ also produced a super warning in 2025; however, this occurred later and was associated solely with B3.13.

These observations suggest that, because of the large number of sequences with incomplete metadata, the patchy distribution and relatively limited number of available sequences starting from February 2025, configurations of stray with ($N = 50$) are better suited for analyzing 2025 data and can effectively flag the D1.1 spillover to dairy cattle.

Data mart–based analysis for individual B3.13 sequences
FluWarning can be applied to surveillance on smaller scales (US States in our dataset, but, in principle, regional surveillance centers); with more granular analysis, stray can be exploited with lower k parameters. When focusing only on B3.13 sequences, a progressive movement of warnings (using $N = 50$ and $k = 1$) is observed in the same biweekly intervals, see Fig. 3D, showing subsequent US maps
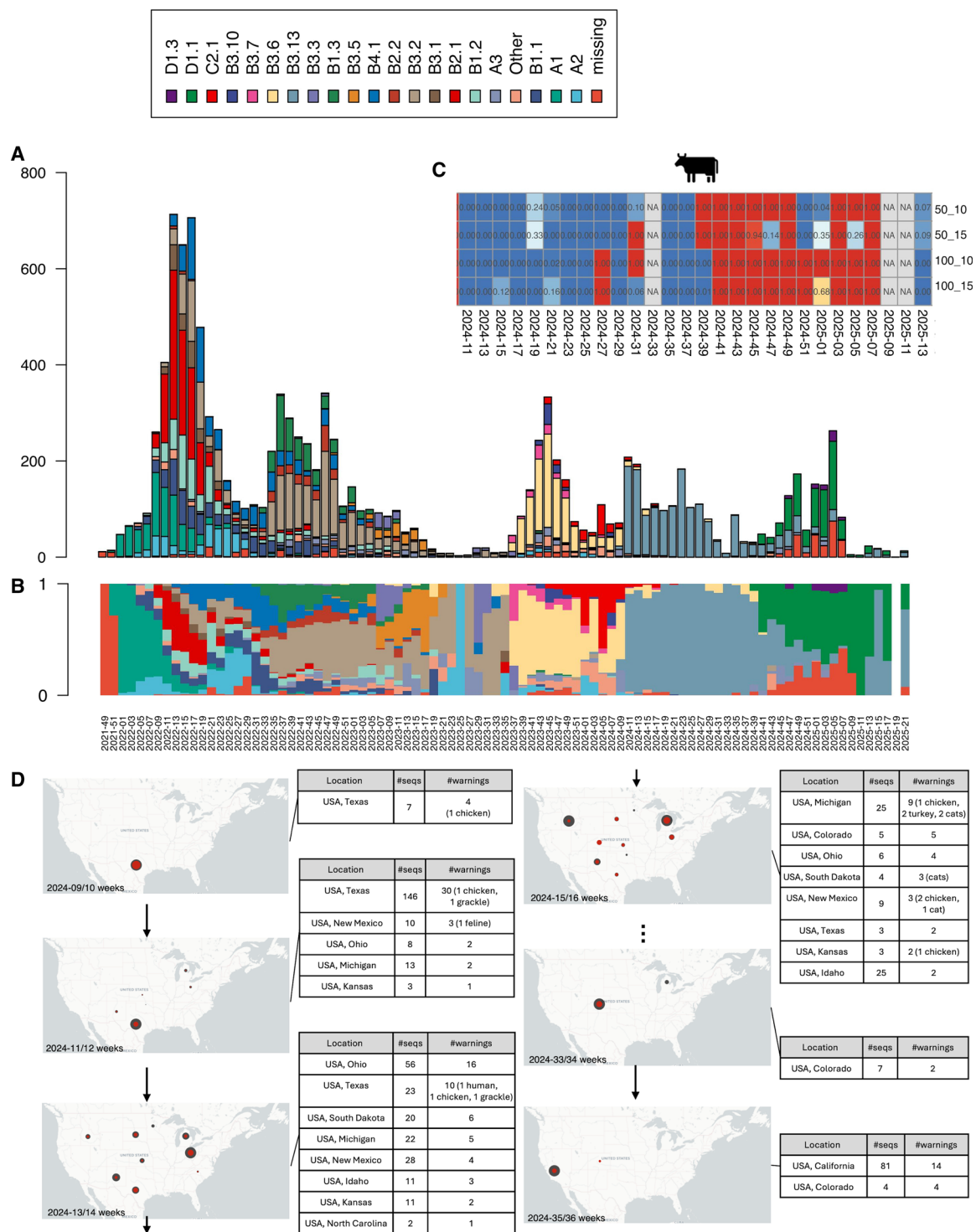
Fig. 3. Circulation of 2.3.4.4b H5N1 strains from 2020 to 2025 and warnings by stray. (**A**) Barplot showing the total number of H5N1 sequences at every time interval, classified according to the genotypes recently associated with H5N1 in North America. (**B**) Relative proportions (percentage with respect to the total number of sequences) of genotypes, shown to facilitate the direct comparison of their prevalence. (**C**) Heatmap displaying the FDR-corrected *P* values for the statistically significant increase in the number of warnings (super warning). Only the interval associated with the diffusion in nonhuman mammals (dairy cattle) is displayed (complete analyses in fig. S5). Time intervals are shown in columns. Parameters of stray on the rows. NA: super warnings were not computed due to an insufficient number of sequences. (**D**) Maps drawn for North and Central America, representing warnings during the 2024-09 to 2024-36 weeks period. One can note the diffusion, initially in Texas (weeks 9 and 10); then also in New Mexico, Ohio, Kansas, and Michigan (weeks 11 and 12); then also in Idaho, North Carolina, and South Dakota (weeks 13 and 14); and then also in Colorado (weeks 15 and 16); we move then to weeks 33 and 36 to show the offspring of warnings in California, first presented in weeks 35 and 36.

and the corresponding B3.13 warning counts (automatically generated by our data mart). Each panel shows geolocated warnings (red circle) included in collected sequences (black circle). Numbers are explicitly indicated in the tables below; gray cards specify warnings thrown by sequences found on hosts other than dairy cows.

Starting 7 March 2024, Texas collected one warning sequence from chicken, then on 10 March 2024, three from dairy cows; the following intervals see an increase in warnings in Texas (one wild bird and one chicken in 2024-12; one human in 2024-13 ID: "EPI_ISL_19027114_A/Texas/37/2024"). At weeks 2024-11/12, we observe warnings in New Mexico (15/16 March), Ohio (15 March), and subsequently Kansas (20 March), New Mexico (feline on 20 March), and Michigan (21 March). In the interval 2024-13/14, warnings were also recorded in Idaho (27 March), North Carolina (4 April), and South Dakota (5 April). In the interval 2024-15/16, warnings appear in Colorado (10 April). The last two maps depict a much later period, showing the emergence of warnings in California (2024-35/36), precisely on August 26th, 2024 (ID: "EPI_ISL_19387789_A/dairy_cow/USA/24_024712–003/2024").

Warnings emitted for 5 US States are shown in fig. S6. For every row, we report biweekly counts, according to all possible assignments of parameters N and k. Note the peculiar situation of California (fig. S6B): Warnings are emitted for a long period, from August 2024 to February 2025, and then very few sequences from complete isolates were collected (seven during biweek starting 24 March 2025 and one during biweek starting 19 May 2025), despite the reported critical situation of dairy cattle (19).

Multisegment analysis

With the aim of assessing whether non-HA segments provide distinct or complementary signals in the identification of divergent/novel viral variants, we applied our early warning system to all eight genomic segments of H5N1 clade 2.3.4.4b. Only viral isolates for which all eight segments of the genome were included in this analysis, for a total of 12,092 viruses. For segments (PB1, PA, MP, and NS) with overlapping coding sequences (CDSs), we considered only the longest CDS. For all the segments, we applied stray with $N = 50$ and $k = 10$, which had previously yielded accurate and timely results for HA.

We compared the overall number of warnings (hundreds per segment) and the number of super warnings derived by the analysis of each segment (Fig. 4A). HA and NA generated a number of super warnings similar to the other segments, but with markedly fewer warnings. While the other segments generally produced approximately one super warning every ~100 warnings, the HA and NA ratios were nearly threefold lower, indicating a more favorable signal-to-noise profile for these two structural segments.

We then inspected the distribution of clade 2.3.4.4b genotypes associated with warnings (Fig. 4B). HA and NA flagged almost exclusively genotype B3.13, whereas the other segments displayed a broader warning profile, encompassing additional genotypes, including B1.1, B1.2, B3.2, and A1, none of which have epidemiological relevance according to current knowledge. Genotypes D1.1 and B3.6 (i.e., the direct ancestor of B3.13) accounted for a relatively small proportion of warnings across all segments, with the exception of the M1 segment, where their representation was slightly elevated.

We computed super warnings over the 2-year interval from week 2023-19 to week 2025-21, spanning the recent spillover of 2.3.4.4b into dairy cattle for all eight segments, and compared their temporal distribution (Fig. 4C). A high degree of concordance was observed among segments, with the majority of super warnings clustered between weeks 2024-11 and 2024-39 and corresponding to the emergence of B3.13. Genotypes associated with every super warning, derived by the analysis of each independent segment, were recorded and inspected.

According to fig. S7, HA primarily flagged B3.13 but also detected B3.6 and D1.1. The latter's super warning occurred in January 2025, coinciding with its independent spillover into dairy cattle, and aligned well with epidemiological observations. NA, NP, and NS1 exhibited temporal and genotype-specific super warning patterns broadly consistent with those detected for HA. Nonetheless, these segments additionally identified genotypes not currently regarded as epidemiologically relevant, including A3 and B3.7 (NP), C2.1 (NS1), and D1.3 (NA). Furthermore, although all three segments generated super warnings for D1.1, in contrast to HA, these signals were distributed across an extended temporal interval and did not temporally coincide with the reported spillover of this lineage into dairy cattle.

Segment M1 (fig. S8) flagged additional nonepidemiologically relevant genotypes (A.3 and C2.1) and detected B3.13 with a delay of 2 weeks compared to HA, whereas it identified B3.6 and D1.1 earlier than HA. Among other segments (fig. S8), PB2 exhibited a limited number of super warnings and did not identify B3.13 in a timely manner. PB1 and PA exhibited a more patchy temporal profile, and their super warnings were linked not only to epidemiologically relevant genotypes but also to A2, C2.1, and other minor genotypes.

Together, these findings support the HA segment as the best single-segment choice for a lightweight warning system. Its advantages include a reduced total number of warnings, robust identification of all currently epidemiologically relevant genotypes in clade 2.3.4.4b, and ease of interpretation, given the large record of potentially epidemiologically relevant mutations already characterized for the HA gene. NA and NP could be viable alternatives, with overall similar performance metrics, but with reduced interpretability compared to HA. In contrast, nonstructural segments (PA, PB2, PB1, and NS1) and the M1 segment are less suitable due to their higher warning counts and the broader spectrum of genotypes, many of which are not epidemiologically relevant, associated with their super warnings. This wider genotype range may reflect higher reassortment rates for these internal proteins, consistent with previous reports of segment-specific reassortment dynamics in H5N* avian influenza viruses (32, 33).

Cluster and mutation analysis

The HaploCoV (34) software was used to partition 2.3.4.4b genotypes, as defined by Nguyen et al. (19), into clusters of similar HA sequences. Distinct clusters were delineated when at least 100 sequences differed by five or more nonshared nucleotide variants. A total of 10 distinct clusters were formed (Fig. 5A). Three of these 10 clusters (HA.N1, HA.N2, and HA.N10) were composed almost exclusively of sequences assigned to the B3.13 genotype. The B3.6 genotype, ancestor of B3.13 according to (19), corresponded with a single HaploCoV cluster labeled HA.N3. All HA segments of genotype D1.1 were assigned to a single HaploCoV cluster (HA.N5).

As observed in fig. S9, the B3.6 (HA.N3) and D1.1 (HA.N5) genotypes were widespread across many states; HA.N1 was associated
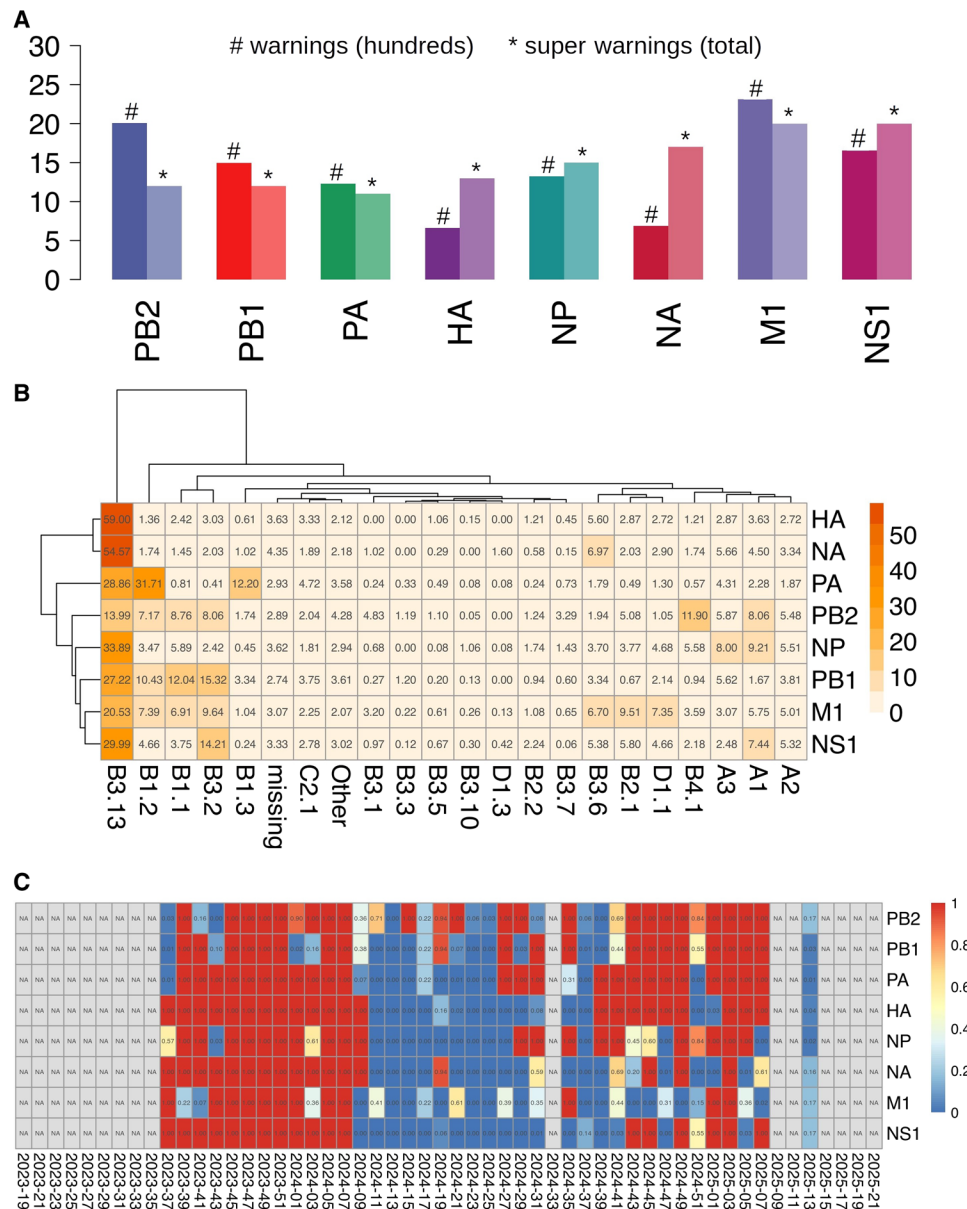
Fig. 4. Comparison of warnings and super warnings obtained from the analysis of all eight segments of H5N1 2.3.4.4b influenza A genomes. (**A**) Barplot showing the total number of warnings (in hundreds, #) and the number of super warnings, displayed side by side for each segment. (**B**) Heatmap illustrating the overall proportion (%) of warnings associated with distinct 2.3.4.4b genotypes for each genome segment. Genotypes are reported on the columns, segments on the rows. A two-way hierarchical clustering groups segments and genotypes with similar patterns of warnings detected by stray. (**C**) Heatmap of super warnings associated with each segment from 2023-19 to 2025-21. Time intervals are shown on the columns and segments on the rows. Corrected P values for super warnings are reported in each cell.

with specimens collected from dairy cattle in Texas, Colorado, Idaho, Michigan, and Minnesota; instead, the HA.N10 and HA.N2 clusters, detected starting from week 2024-35, were observed only in California.

We designate as defining nucleotide variants those observed in at least 50% of the sequences of each HaploCoV cluster; these nucleotide variants were inspected (see Fig. 5B). Consistent with phylogenetic analyses, HA.N3 (B3.6) and HA.N1, HA.N10, and HA.N2 (B3.13) shared a similar pattern of defining nucleotide variants and formed a well-defined group. HA.N1, HA.N10, and HA.N2 displayed five additional characteristic nucleotide variants compared

to HA.N3; none of them resulted in an amino acid substitution. However, HA.N2 and HA.N10 displayed two additional nonsynonymous substitutions, i.e., S336N and D104G, compared to HA.N1. S336N was previously reported as a virulence marker, with an increased prevalence in viruses isolated from dairy cows (19). D104G was recently associated with a marked increase in immune escape (35). Genotype D1.1 (HA.N5) exhibited a mutational profile closely related to that of genotype A3 (HA.N11), consistent with the known evolutionary history of these lineages (36). However, D1.1 displayed two additional characteristic amino acid changes: T52A in the H1 segment and N146D in the H2 segment. To date, neither of these
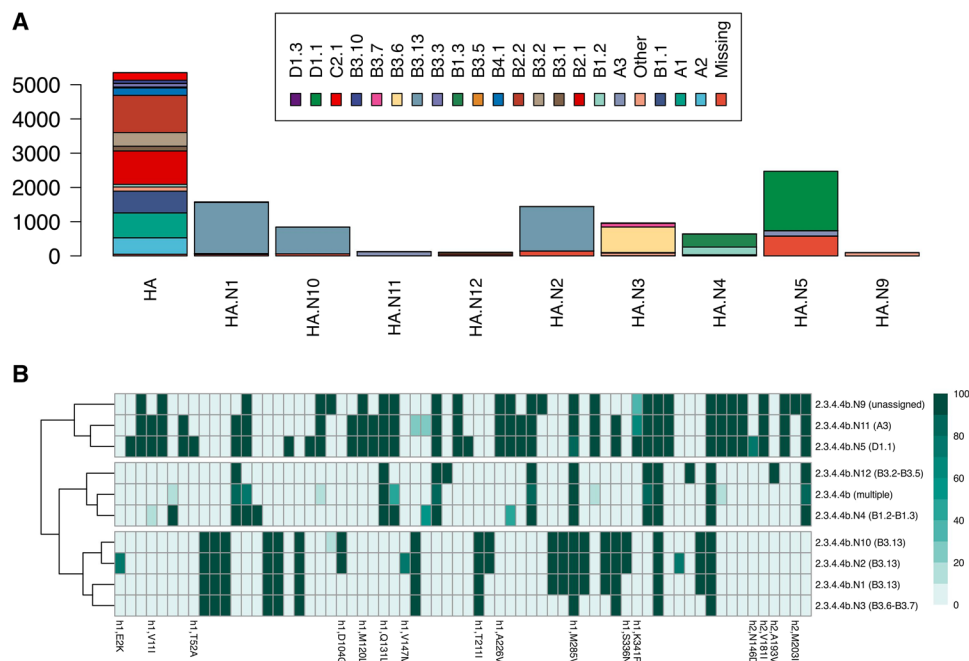
Fig. 5. Number of sequences of each genotype corresponding to a HaploCoV-defined cluster and characteristic mutations of HaploCoV clusters. (**A**) For every HaploCoV cluster, the barplot displays the total number of sequences from each distinct genotype assigned to that cluster. Clusters HA.N1, HA.N10, and HA.N2 are formed almost exclusively by sequences assigned to the B3.13 genotype. Similarly, a clear correspondence between HA.N3 and B3.6 can be observed. (**B**) The heatmap illustrates the prevalences (% min 0 max 100) of characteristic nucleotide variants in each distinct HaploCoV cluster. HaploCoV clusters are reported on the columns; nucleotide variants on the rows. For nucleotide variants associated with nonsynonymous substitutions, the predicted amino acid substitution is reported (complete annotation in data S1). Consistent with phylogenetic analyses, clusters associated with B3.6 (HA.N3) and B3.13 (HA.N1, HA.N10, and HA.N2) form a neat and well-separated group and are defined by a similar pattern of characteristic nucleotide variants.

mutations has been associated with any known functional or epidemiological relevance. Together, these analyses provide preliminary evidence of potential host adaptation of the B3.13 lineage in dairy cows in California and highlight specific HA mutations in the D1.1 lineage that warrant further investigation.

DISCUSSION

Our FluWarning method issues warnings whenever a new viral sequence is significantly different from a baseline of N previously collected background sequences; differences are measured in a dimensional space of 75 variables, describing dinucleotide frequencies and codon preferences. The method does not differentiate among warnings; these may reflect spillovers, new clades, or new lineages. Investigation responsibility is passed to users who interpret the warning. The method does not make use of phylogenetic analysis but leverages compositional properties of genomes. This makes it able to scale up to big datasets, being computationally faster and generally very accurate, a similar approach has been proven successful in previous research (37–39) that allowed us to detect major evolutionary changes (e.g., variants and recombinations) in SARS-CoV-2 genomes.

The method is multiscale, as it considers different levels of alerting: simple warnings are issued on single sequences (that may be anomalous in groups of k elements); super warnings are based on biweekly batches of collected sequences and require a statistically significant size and P value. Simple warnings can be observed on different location scales, host populations, and genotypes, while super warnings are available at the whole-dataset level (but could be adapted to different scales). We illustrated the robustness of the method by computing sensitivity and specificity with increasing amounts of noise, starting from an ideal case of replacement of a baseline population by a new viral population.

While multiple genome segments can yield timely and informative signals, the HA segment alone provides an efficient, interpretable, and high-specificity basis for a lightweight genomic surveillance tool, such as FluWarning. Expanding surveillance to multiple segments may still offer incremental benefits, in particular for capturing early reassortment events or detecting rare genotype emergences, but would entail a higher noise level and analytic complexity.

FluWarning is conceived for supporting surveillance systems that sample domestic and wild animals globally; it is most likely to succeed when applied to pathogens with an existing surveillance network (now in place only for seasonal influenza). Even under the best surveillance systems (like the WHO's seasonal influenza GISRS system), sequences routinely get backfilled for earlier dates after the sample collection. Therefore, should public health officials run FluWarning over public data, the input would be relatively incomplete and noisy.

Thanks to its lightweight code, user-defined parametrization, and easy-to-inspect data mart analytics, FluWarning has the potential of being used by many laboratories or regional-scale genomic surveillance institutions. The accuracy of our tool shows that broader and deeper support for global surveillance could pay off, enabling substantial small-scale discoveries.

MATERIALS AND METHODS

Data collection and genome quality filtering

We download from GISAID EpiFlu (*10*) two sets of sequences and their metadata: (i) the H1N1 sequences deposited in North America from mammalian hosts between the 28 July 2008 and 10 January 2010; and (ii) the H5N1 sequences deposited in North America from all available hosts between 1 January 2019 and 25 July 2025 (however, no North American sequences with complete collection date metadata were deposited after 29 May). For each isolate of H1N1, we require the HA segment to be available and complete. For each isolate of H5N1, we require all segments to be available and complete.

The two sets count 3387 and 12,854 sequences, respectively. Our data cleaning pipeline removes the sequences with a percentage of unknown nucleotide bases >2%, duplicate Isolate_ID and Isolate_Name, incomplete Collection_Date, or whose length is >±7% dissimilar from the mode. Then, we extract the CDS of the relevant proteins, and assign each codon with the corresponding amino acid according to the genetic code; we remove those sequences with incomplete or truncated CDS (i.e., when the length is not a multiple of 3). After this pipeline, we obtain 3034 HA sequences for H1N1 and 12,092 sequences of all segments for H5N1.

The distribution of host species shows that 96.4% of the H1N1 sequences are from human hosts and the remaining 3.6% (146 sequences) from swine. For H5N1 sequences, 79.6% of the sequences are collected from wild birds, 5.9% from domestic birds, 14.2% from nonhuman mammals, and 0.3% from human hosts.

Data processing

The data processing pipeline extracts an array of 75 numeric features from the CDS of each input sequence. The first set of features is the logarithm of the RSCU (*26*), which is computed for all codons except three stop codons (TAA, TAG, and TGA) and two nonsynonymous codons (ATG and TGG). This leads to 59 log-RSCU values for each CDS, computed as in Eq. 1, where X_{ij} is the frequency of the codon jth encoding the ith amino acid, and n_i is the number of synonymous codons encoding the jth amino acid. The RSCU allows us to measure the over/under usage of a codon within a genomic sequence, assuming even codon usage between synonymous codons as a baseline value. One common pitfall of the RSCU is that the values representing under-usage are shrunk between 0 and 1, while those representing over can reach values well beyond 2 or 3. To balance the range of values for expressing the under/overusage, the RSCU is transformed through the logarithm function to base n_i.

$$\text{log-RSCU}(j) = \log_{n_i}\left(\frac{X_{ij}}{\frac{1}{n_i}\sum_{j=1}^{n_i} X_{ij}} \right) \quad (1)$$

The second set of features derives from the dinucleotide frequencies of all the permutations $P(4, 2)$ with repetitions of the four nucleotides in each CDS sequence. We report the formula in Eq. 2 for the permutation C, A in a CDS of length N; a $\log_2$ transformation is applied to homogenize the values with those of log-RSCU.

$$\text{log-dinucleotide}(C, A) = \log_2\left(\frac{\frac{\text{count}(C,A)}{N-1}}{\frac{\text{count}(C)*\text{count}(A)}{N^2}} \right) \quad (2)$$

More details on stray

The stray method is an improved variant of the HDoutlier method (*40*). Essentially, while HDoutlier uses neighbor distance to identify outliers, stray uses the k-neighbor distance, thus allowing microclusters of outliers of size $k - 1$. In addition, it provides a data-driven threshold for anomaly detection. Some aspects of the stray method require further explanation. First, as variables with large variance can have a disproportional influence on Euclidean distance calculation (*40*), the input features for stray are normalized between [0, 1] through a standard min-max scaler right before running the outlier detection algorithm.

The anomalous threshold calculation is an application of Weissman's spacing theorem (*41*) that applies to data distributions covered by the maximum domain of attraction of a Gumbel distribution; note that this requirement is satisfied by a wide range of distributions, including the exponential, γ, normal and log-normal distributions with exponentially decaying tails (*9*). For the threshold calculation, stray adopts the "bottom-up searching algorithm" defined in (*42*); the threshold calculation is performed under the assumption that the distribution of k-nearest neighbors with the maximum gap is in the maximum domain of attraction of the Gumbel distribution.

For simplicity, we consider as output a binary classification; the stray algorithm may also assign an anomalous score to each data instance. The method considers totally ordered data streams for optimizing the coding of the stray algorithm (*43*). Our dataset is totally ordered by ⟨depositionTime,isolateID⟩, fitting the stray input requirements.

Identification of super warnings

Intervals of time associated with a significant increase in the number of warnings were identified by a one-sided Fisher's exact test. In brief, for every window W_i, a 2 × 2 contingency table was built by recording, in column 1, the total number of warning and nonwarning sequences in the window, and in column 2 the equivalent counts across the complete dataset excluding W_i. Counts in row 1 represent the total number of sequences labeled as warnings, whereas counts in row 2 represent the total number of sequences not labeled as warnings. The test statistics and the P value were computed by the fisher.test() function as implemented by the stats package in R. Correction for multiple testing was computed by the p.adjust() function from the same software library. Simulations of corrected P values under varying numbers of available sequences and proportions of warning sequences were performed in R using the same functions applied to in silico contingency tables. The values in column 1 were computed according to the specified number of sequences and proportion of warnings. In p.adjust(), the parameter n (number of tests to correct for) was set to the total number of time windows in the original dataset.

Clusters of HA sequences and characteristic mutations

The HaploCoV software (*34*) was used to identify groups (clusters) of sequences that share common patterns of nucleotide variants in the HA segment of H5N1. HaploCoV detects clusters consisting of at least a user-specified minimum number of sequences (*S*), each containing at least *N* high-frequency nucleotide variants (with a frequency of occurrence in the dataset ≥1%) not shared with any other group. In this analysis, the parameters were set as $S = 100$ and $N = 5$.

Each cluster is labeled with the prefix .N, followed by a sequential number. Following the approach in (*19*), the PQ705761 sequence (GenBank accession) was used as the reference sequence for the

identification of nucleotide variants. For every cluster, characteristic mutations were defined as those observed in at least 50% of the sequences assigned to a clade/subclade.

Data mart implementation

Fifteen configurations of stray, obtained by setting N and k parameters, are run on the full dataset extracted as described in the "Data collection and genome quality filtering" section. For each configuration, FluWarning has been run on N-sized windows, progressively acquiring a new sequence and dropping a previous sequence, following a complete order built by CollectionDate and then AccessionId. The outputs of each run (each resulting in either 0 or 1 warning) are aggregated in macrowindows of 2 weeks, by summing the number of runs that output one warning (see Results, H1N1). Biweekly counts of warnings make results more readable and applicable to practical, real-world scenarios. These aggregations are stored, generating a large data mart (16). While the method is run on the whole dataset, results can be projected on subsets of sequences corresponding, e.g., to specific host types, geographical locations, and time intervals (e.g., sequences collected in Canada or Massachusetts for Swine hosts in the interval March 2009 to Sept 2009). Counts are evaluated as absolute values or as percentages of warnings in the observed bi-weekly period. The selected data structure allows us to quickly navigate the number of runs that have been generated by FluWarning. Most notably, it allows us to keep an up-to-date visual representation (e.g., on geographical maps) of how warnings are distributed worldwide and how they evolve along biweekly intervals.

Supplementary Materials
The PDF file includes:
Table S1
Figs. S1 to S9
Legend for dataset S1

Other Supplementary Material for this manuscript includes the following:
Dataset S1

REFERENCES AND NOTES
1. A. J. Meadows, N. Stephenson, N. K. Madhav, B. Oppenheim, Historical trends demonstrate a pattern of increasingly frequent and severe spillover events of high-consequence zoonotic viruses. *BMJ Glob. Health* **8**, e012026 (2023).
2. S. Mursel, N. Alter, L. Slavit, A. Smith, P. Bocchini, J. Buceta, Estimation of Ebola's spillover infection exposure in Sierra Leone based on sociodemographic and economic factors. *PLOS ONE* **17**, e0271886 (2022).
3. G. T. Keusch, J. H. Amuasi, D. E. Anderson, P. Daszak, I. Eckerle, H. Field, M. Koopmans, S. K. Lam, C. G. das Neves, M. Peiris, S. Perlman, S. Wacharapluesadee, S. Yadana, L. Saif, Pandemic origins and a One Health approach to preparedness and prevention: Solutions based on SARS-CoV-2 and other RNA viruses. *Proc. Natl. Acad. Sci. U.S.A.* **119**, e2202871119 (2022).
4. V. Chandola, A. Banerjee, V. Kumar, Anomaly detection: A survey. *ACM Comput. Surv.* **41**, 1–58 (2009).
5. C. C. Aggarwal, *Otlier analysis* (2nd ed.) (Cham: Springer, 2017).
6. M. Gupta, J. Gao, C. C. Aggarwal, J. Han, Outlier detection for temporal data: A survey. *IEEE Trans. Knowl. Data Eng.* **26**, 2250–2267 (2014).
7. E. H. Wong, D. K. Smith, R. Rabadan, M. Peiris, L. L. Poon, Codon usage bias and the evolution of influenza A viruses. Codon usage biases of influenza virus. *BMC Evol. Biol.* **10**, 253 (2010).
8. T. Alfonsi, M. Chiara, A. Bernasconi, A codon usage-based approach for the stratification of influenza A across recent spillovers. *Comput. Struct. Biotechnol. J.* **27**, 2757–2771 (2025).
9. P. D. Talagala, R. J. Hyndman, K. Smith-Miles, Anomaly detection in high-dimensional data. *J. Comput. Graph. Stat.* **30**, 360–374 (2021).
10. Y. Shu, J. McCauley, GISAID: Global Initiative on Sharing All Influenza Data–From vision to reality. *Euro Surveill.* **22**, 30494 (2017).
11. A. Gambaryan, A. Tuzikov, G. Pazynina, N. Bovin, A. Balish, A. Klimov, Evolution of the receptor binding phenotype of influenza A (H5) viruses. *Virology* **344**, 432–438 (2006).
12. Y. Turakhia, B. Thornlow, A. Hinrichs, J. McBroome, N. Ayala, C. Ye, K. Smith, N. de Maio, D. Haussler, R. Lanfear, R. Corbett-Detig, Pandemic-scale phylogenomics reveals the SARS-CoV-2 recombination landscape. *Nature* **609**, 994–997 (2022).
13. A. Forna, K. B. Weedop, L. Damodaran, N. Hassell, R. Kondor, J. Bahl, J. M. Drake, P. Rohani, Sequence-based detection of emerging antigenically novel influenza A viruses. *Proc. Biol. Sci.* **291**, 20240790 (2024).
14. A. Garjani, A. M. Chegini, M. Salehi, A. Tabibzadeh, P. Yousefi, M. H. Razizadeh, M. Esghaei, M. Esghaei, M. H. Rohban, Forecasting influenza hemagglutinin mutations through the lens of anomaly detection. *Sci. Rep.* **13**, 14944 (2023).
15. T. Alfonsi, A. Bernasconi, M. Chiara, S. Ceri, Supporting data and code for "Lightweight multi-scale early warning system for influenza A spillovers". https://doi.org/10.5281/zenodo.15498406.
16. A. Bonifati, F. Cattaneo, S. Ceri, A. Fuggetta, S. Paraboschi, Designing data marts for data warehouses. *ACM Trans. Softw. Eng. Methodol.* **10**, 452–483 (2001).
17. L. C. Caserta, E. A. Frye, S. L. Butt, M. Laverack, M. Nooruzzaman, L. M. Covaleda, A. C. Thompson, M. P. Koscielny, B. Cronk, A. Johnson, K. Kleinhenz, E. E. Edwards, G. Gomez, G. Hitchener, M. Martins, D. R. Kapczynski, D. L. Suarez, E. R. A. Morris, T. Hensley, J. S. Beeby, M. Lejeune, A. K. Swinford, F. Elvinger, K. M. Dimitrov, D. G. Diel, Spillover of highly pathogenic avian influenza H5N1 virus to dairy cattle. *Nature* **634**, 669–676 (2024).
18. D. M. Morens, J. Park, J. K. Taubenberger, Many potential pathways to future pandemic influenza. *Sci. Transl. Med.* **15**, eadj2379 (2023).
19. T.-Q. Nguyen, C. R. Hutter, A. Markin, M. Thomas, K. Lantz, M. L. Killian, G. M. Janzen, S. Vijendran, S. Wagle, B. Inderski, D. R. Magstadt, G. Li, D. G. Diel, E. A. Frye, K. M. Dimitrov, A. K. Swinford, A. C. Thompson, K. R. Snekvik, D. L. Suarez, S. M. Lakin, S. Schwabenlander, S. C. Ahola, K. R. Johnson, A. L. Baker, S. Robbe-Austerman, M. K. Torchetti, T. K. Anderson, Emergence and interstate spread of highly pathogenic avian influenza A(H5N1) in dairy cattle in the United States. *Science* **388**, eadq0900 (2025).
20. Y. Iwasaki, T. Abe, Y. Wada, K. Wada, T. Ikemura, Novel bioinformatics strategies for prediction of directional sequence changes in influenza virus genomes and for surveillance of potentially hazardous strains. *BMC Infect. Dis.* **13**, 386 (2013).
21. S. A. Babayan, R. J. Orton, D. G. Streicker, Predicting reservoir hosts and arthropod vectors from evolutionary signatures in RNA virus genomes. *Science* **362**, 577–580 (2018).
22. H. Deka, S. Chakraborty, Compositional constraint is the key force in shaping codon usage bias in hemagglutinin gene in H1N1 subtype of influenza A Virus. *Int. J. Genomics* **2014**, 349139 (2014).
23. H. Gu, R. L. Fan, D. Wang, L. L. Poon, Dinucleotide evolutionary dynamics in influenza A virus. *Virus Evol.* **5**, vez038 (2019).
24. J. Sun, W. Zhao, R. Wang, W. Zhang, G. Li, M. Lu, Y. Shao, Y. Yang, N. Wang, Q. Gao, S. Su, Analysis of the codon usage pattern of HA and NA genes of H7N9 influenza A virus. *Int. J. Mol. Sci.* **21**, 7129 (2020).
25. J. Li, S. Zhang, B. Li, Y. Hu, X. P. Kang, X. Y. Wu, M. T. Huang, Y. C. Li, Z. P. Zhao, C. F. Qin, T. Jiang, Machine learning methods for predicting human-adaptive influenza a viruses based on viral nucleotide compositions. *Mol. Biol. Evol.* **37**, 1224–1236 (2020).
26. P. M. Sharp, W.-H. Li, An evolutionary perspective on synonymous codon usage in unicellular organisms. *J. Mol. Evol.* **24**, 28–38 (1986).
27. I. Mena, M. I. Nelson, F. Quezada-Monroy, J. Dutta, R. Cortes-Fernández, J. H. Lara-Puente, F. Castro-Peralta, L. F. Cunha, N. S. Trovão, B. Lozano-Dubernard, A. Rambaut, H. van Bakel, A. García-Sastre, Origins of the 2009 H1N1 influenza pandemic in swine in Mexico. *eLife* **5**, e16777 (2016).
28. M. P. Girard, J. S. Tam, O. M. Assossou, M. P. Kieny, The 2009 A (H1N1) influenza virus pandemic: A review. *Vaccine* **28**, 4895–4902 (2010).
29. T. P. Peacock, L. Moncla, G. Dudas, D. VanInsberghe, K. Sukhova, J. O. Lloyd-Smith, M. Worobey, A. C. Lowen, M. I. Nelson, The global H5N1 influenza panzootic in mammals. *Nature* **637**, 304–313 (2025).
30. A. Fusaro, B. Zecchin, E. Giussani, E. Palumbo, M. Agüero-García, C. Bachofen, Á. Bálint, F. Banihashem, A. C. Banyard, N. Beerens, M. Bourg, F.-X. Briand, C. Bröjer, I. H. Brown, B. Brugger, A. M. P. Byrne, A. Cana, V. Christodoulou, Z. Dirbakova, T. Fagulha, R. A. M. Fouchier, L. Garza-Cuartero, G. Georgiades, B. Gjerset, B. Grasland, O. Groza, T. Harder, A. M. Henriques, C. K. Hjulsager, E. Ivanova, Z. Janeliunas, L. Krivko, K. Lemon, Y. Liang, A. Lika, P. Malik, M. J. McMenamy, A. Nagy, I. Nurmoja, I. Onita, A. Pohlmann, S. Revilla-Fernández, A. Sánchez-Sánchez, V. Savic, B. Slavec, K. Smietanka, C. J. Snoeck, M. Steensels, V. Svansson, E. Swieton, N. Tammiranta, M. Tinak, S. Van Borm, S. Zohari, C. Adlhoch, F. Baldinelli, C. Terregino, I. Monne, High pathogenic avian influenza A (H5) viruses of clade 2.3.4.4b in Europe–Why trends of virus evolution are more difficult to predict. *Virus Evol.* **10**, veae027 (2024).
31. Animal and Plant Health Inspection Service - U.S. Department of Agriculture, APHIS Confirms D1.1 Genotype in Dairy Cattle in Nevada. https://www.aphis.usda.gov/news/program-update/aphis-confirms-d11-genotype-dairy-cattle-nevada-0.

32. L. Lu, S. J. Lycett, A. J. Leigh Brown, Reassortment patterns of avian influenza virus internal segments among different subtypes. *BMC Evol. Biol.* **14**, 16 (2014).

33. D. He, X. Wang, H. Wu, X. Wang, Y. Yan, Y. Li, T. Zhan, X. Hao, J. Hu, S. Hu, X. Liu, C. Ding, S. Su, M. Gu, X. Liu, Genome-wide reassortment analysis of influenza a H7N9 viruses circulating in China during 2013–2019. *Viruses* **14**, 1256 (2022).

34. M. Chiara, D. S. Horner, E. Ferrandi, C. Gissi, G. Pesole, HaploCoV: Unsupervised classification and rapid detection of novel emerging variants of SARS-CoV-2. *Commun. Biol.* **6**, 443 (2023).

35. K. Miyakawa, M. Ota, K. Sano, F. Momose, N. Kishida, T. Arita, Y. Suzuki, M. Shirakura, H. Asanuma, S. Watanabe, H. Hasegawa, Emergence of antigenic variants in bovine H5N1 influenza viruses. *J. Med. Virol.* **97**, e70394 (2025).

36. A. Mostafa, A. Nogales, L. Martinez-Sobrido, Highly pathogenic avian influenza H5N1 in the United States: Recent incursions and spillover to cattle. *NPJ Viruses* **3**, 54 (2025).

37. A. Bernasconi, L. Mari, R. Casagrandi, S. Ceri, Data-driven analysis of amino acid change dynamics timely reveals SARS-CoV-2 variant emergence. *Sci. Rep.* **11**, 21068 (2021).

38. P. Pinoli, A. Canakoglu, S. Ceri, M. Chiara, E. Ferrandi, L. Minotti, A. Bernasconi, VariantHunter: A method and tool for fast detection of emerging SARS-CoV-2 variants. *Database* **2023**, baad044 (2023).

39. T. Alfonsi, A. Bernasconi, M. Chiara, S. Ceri, Data-driven recombination detection in viral genomes. *Nat. Commun.* **15**, 3313 (2024).

40. L. Wilkinson, Visualizing big data outliers through distributed aggregation. *IEEE Trans. Vis. Comput. Graph.* **24**, 256–266 (2018).

41. I. Weissman, Estimation of parameters and large quantiles based on the k largest observations. *J. Am. Stat. Assoc.* **73**, 812–815 (1978).

42. K. T. Schwarz, *Wind Dispersion of Carbon Dioxide Leaking From Underground Sequestration, and Outlier Detection in Eddy Covariance Data Using Extreme Value Theory* (University of California, Berkeley, 2008).

43. SKTime, STRAY, https://www.sktime.net/en/v0.31.0/api_reference/auto_generated/sktime.annotation.stray.STRAY.html. [accessed 24 Aug 2025].